

# Spatially extended K I $\lambda 7699$ emission in the nebula of VY CMa: Kinematics and geometry

Nathan Smith<sup>\*†</sup>

*Center for Astrophysics and Space Astronomy, University of Colorado, 389 UCB, Boulder, CO 80309, USA*

Accepted 0000, Received 0000, in original form 0000

## ABSTRACT

Long-slit echelle spectra reveal bright extended emission from the K I  $\lambda 7699$  resonance line in the reflection nebula surrounding the extreme red supergiant VY Canis Majoris. The central star has long been known for its unusually-bright K I emission lines, but this is the first report of intrinsic emission from K I in the nebula. The extended emission is not just a reflected spectrum of the star, but is due to resonant scattering by K atoms in the outer nebula itself, and is therefore a valuable probe of the kinematics and geometry of VY CMa’s circumstellar environment. Dramatic velocity structure is seen in the long-slit spectra, and most lines of sight through the nebula intersect multiple distinct velocity components. A faint “halo” at large distances from the star does appear to show a reflected spectrum, however, and suggests a systemic velocity of  $+40 \text{ km s}^{-1}$  with respect to the Sun. The most striking feature is blueshifted emission from the filled interior of a large shell seen in images; the kinematic structure is reminiscent of a Hubble flow, and provides strong evidence for asymmetric and episodic mass loss due to localized eruptions on the star’s surface.

**Key words:** circumstellar matter — stars: evolution — stars: individual (VY CMa) — stars: mass-loss

## 1 INTRODUCTION

Due to enhanced mass loss during the final stages of stellar evolution, red supergiants are surrounded by extended gas and dust envelopes. This material forms the pre-supernova circumstellar environment, or may get swept-up to form a ring nebula if the star evolves blueward to become a luminous blue variable or Wolf-Rayet star. In a brief phase when mass-loss peaks, these stars can have circumstellar nebulae dense enough to emit OH masers and strong thermal infrared (IR) emission from dust that may obscure the star (OH/IR stars). Among the most luminous red supergiants above  $10^{5.5} L_{\odot}$ , only a handful in our Galaxy are OH/IR stars — one of the most luminous is the M5e Ia supergiant VY Canis Majoris. At a distance of 1.5 kpc (Herbig 1972; Lada & Reid 1978; Marvel 1997), its luminosity is  $10^{5.7} L_{\odot}$ .

VY CMa is a special case among the most luminous red supergiants, because of its spectacular reflection nebula, with strong polarization (Herbig 1972) and intricate knotty and filamentary structure seen in *Hubble Space Telescope* (*HST*) and ground-based IR images (Kastner & Weintraub

1998; Monnier et al. 1999; Smith et al. 2001). These studies revealed a chaotic and highly asymmetric distribution of dust in the circumstellar environment. VY CMa also has strong SiO, H<sub>2</sub>O, and OH maser emission (Knowles et al. 1969; Buhl et al. 1974). Proper motions and Doppler shifts of these masers have repeatedly been interpreted to suggest that VY CMa is surrounded by an expanding disk-like distribution of material with the polar axis oriented northeast-southwest (van Blerkom & Auer 1976; Rosen et al. 1978; Benson & Mutel 1979, 1982; Morris & Bowers 1980; Bowers et al. 1983; Deguchi et al. 1983; Richards et al. 1998). These maser studies only probe material close to the star, and seem hard to reconcile with the severely asymmetric arrangement of knots, arcs, and chaotic filaments seen at larger radii in optical *HST* images (Smith et al. 2001; see Figure 1), or the asymmetric structure near the star in the IR (Monnier et al. 1999). A disk-like geometry implies axial symmetry, so perhaps the receding part of the nebula is obscured by foreground material. Nebulae around red supergiants are neutral dusty reflection nebulae, without convenient diagnostics of the geometry and kinematics like the bright H $\alpha$  or [N II] lines commonly used in studies of nebulae around hot stars.

Spectroscopically, VY CMa is unique among red supergiants because the resonance lines of K I  $\lambda 7665$  and  $\lambda 7699$  are seen strongly in emission (Wallerstein 1958; Humphreys

\* Hubble Fellow; nathans@casa.colorado.edu

† Visiting Astronomer at the New Technology Telescope of the European Southern Observatory, La Silla, Chile.

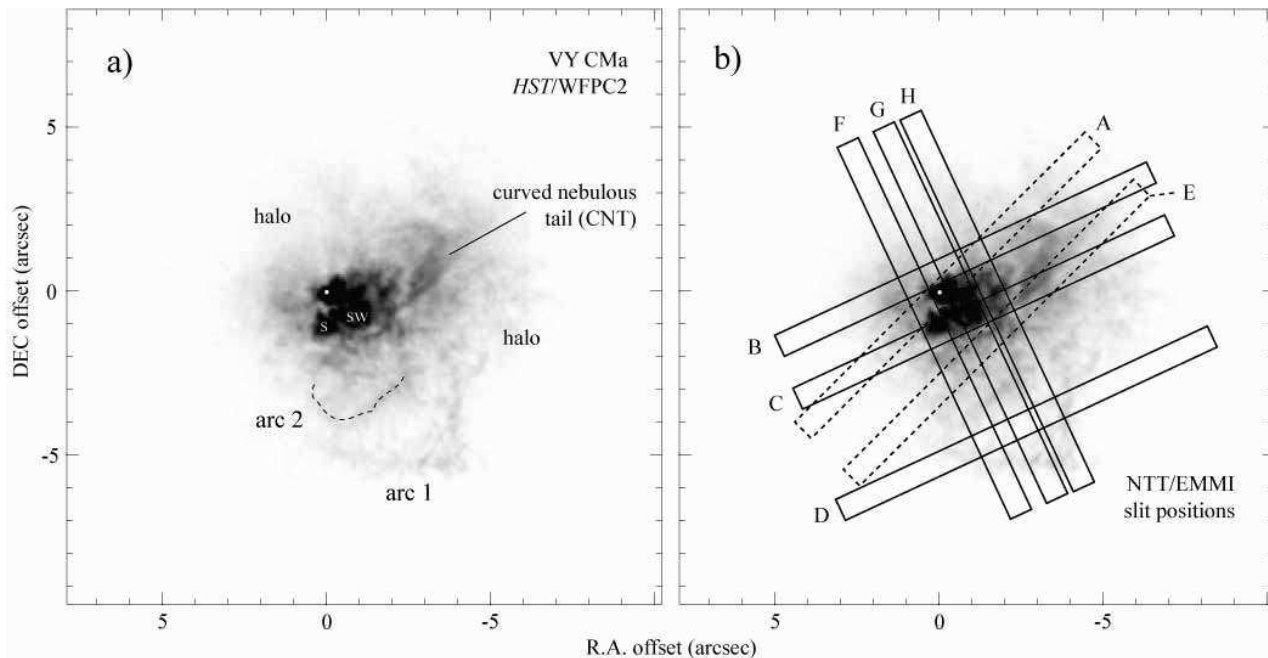


**Figure 1.** Visual-wavelength *HST*/WFPC2 image of VY CMa from Smith et al. (2001), except that here unsharp masking has been applied. Several features discussed in the text are labeled in (a), and (b) shows the positions and orientations of EMMI long-slit aperture positions superposed on the same image of the nebula. Letters A through H correspond to position-velocity diagrams in individual panels of Figure 2, where the position of the letter relative to the slit corresponds to the top of each panel. The small white dot marks the position of the star at visual wavelengths, but the true position of the star is offset slightly to the northeast (Smith et al. 2001; Kastner & Weintraub 1998). Color images showing the outer structure in more detail were published by Smith et al. (2001).

1970; Wallerstein & Gonzalez 2001), accompanied by P Cygni absorption. The K I lines arise in cool gas at  $\sim 700$  to 1000 K (Wallerstein 1958), comparable to dust temperatures near the star (Monnier et al. 1999; Smith et al. 2001). Its spectrum is also unusual in that it shows emission from TiO, ScO, Ti I, Cr I, Rb I, Ba II, etc. (Joy 1942; Wallerstein 1958, 1986; Hyland et al. 1969; Wallerstein & Gonzalez 2001). Emission from the K I lines is sometimes seen in extended envelopes of red supergiants, including Betelgeuse (Bernat & Lambert 1976; Bernat et al. 1978; Mauron et al. 1984; Plez & Lambert 1994, 2002), but the extreme strength of K I emission in the spectrum of the central star is rare.

This Letter reports the discovery that the previously-known K I emission in the star’s spectrum is accompanied by bright *extended* K I emission from VY CMa’s nebula. The K I lines are by far the brightest emission lines throughout the IR and visual-wavelength spectrum of the nebula. K I emission traces roughly the same spatial extent as the reflection nebula, and yields interesting clues to the kinematics and geometry of VY CMa’s circumstellar environment.

## 2 OBSERVATIONS

High-resolution optical spectra of VY CMa were obtained at the European Southern Observatory (ESO) at La Silla, Chile on the nights of 8, 10, and 11 March 2003 using the ESO Multi-Mode Instrument (EMMI) on the New Technology Telescope (NTT). Cross-dispersed echelle spectra were obtained using EMMI’s red CCD (a  $4096 \times 4096$  pixel MIT/LL detector) with the number 10 echelle grating and grism 6

**Table 1.** Spectroscopic Observations of VY CMa

Slit	Date d/m/y	P.A. (deg)	Exp. (min)	Comment
A	8/3/03	135	9	star
B	11/3/03	295	30	offset N, CNT
C	11/3/03	295	30	offset S, CNT
D	11/3/03	295	30	offset S, arc1
E	8/3/03	135	30	CNT and arc2
F	10/3/03	205	30	offset E, arc2
G	10/3/03	205	9	offset W, knots, arc1
H	10/3/03	205	30	offset W, arc1

for order separation. The separation between adjacent orders on the CCD allows for some spatial information to be recorded with a  $\sim 13''$  long slit aperture; this is well-suited to VY CMa’s compact reflection nebula (Figure 1). On all three observing nights the seeing was quite good, varying from  $0''.6$  to  $0''.8$  on average. To sample this good seeing and to maximize spectral resolution, a narrow  $0''.8$ -wide slit aperture was used. This configuration yielded a spectral resolution of  $R = \lambda/\Delta\lambda \approx 35,000$  ( $8 \text{ km s}^{-1}$ ), and a pixel scale of  $0''.166 \times 0.0517 \text{ \AA}$  (or  $\sim 2 \text{ km s}^{-1}$  at a wavelength of  $7699 \text{ \AA}$ ). Wavelength calibration was accomplished using observations of an internal emission lamp; heliocentric velocities for the K I  $\lambda 7699$  line are quoted here. Several different slit positions and orientations were used to sample the spectrum of various features seen in images, as shown in Figure 1b. Discussion in this Letter is limited to the velocity structure of the very bright K I  $\lambda 7699$  emission line, since

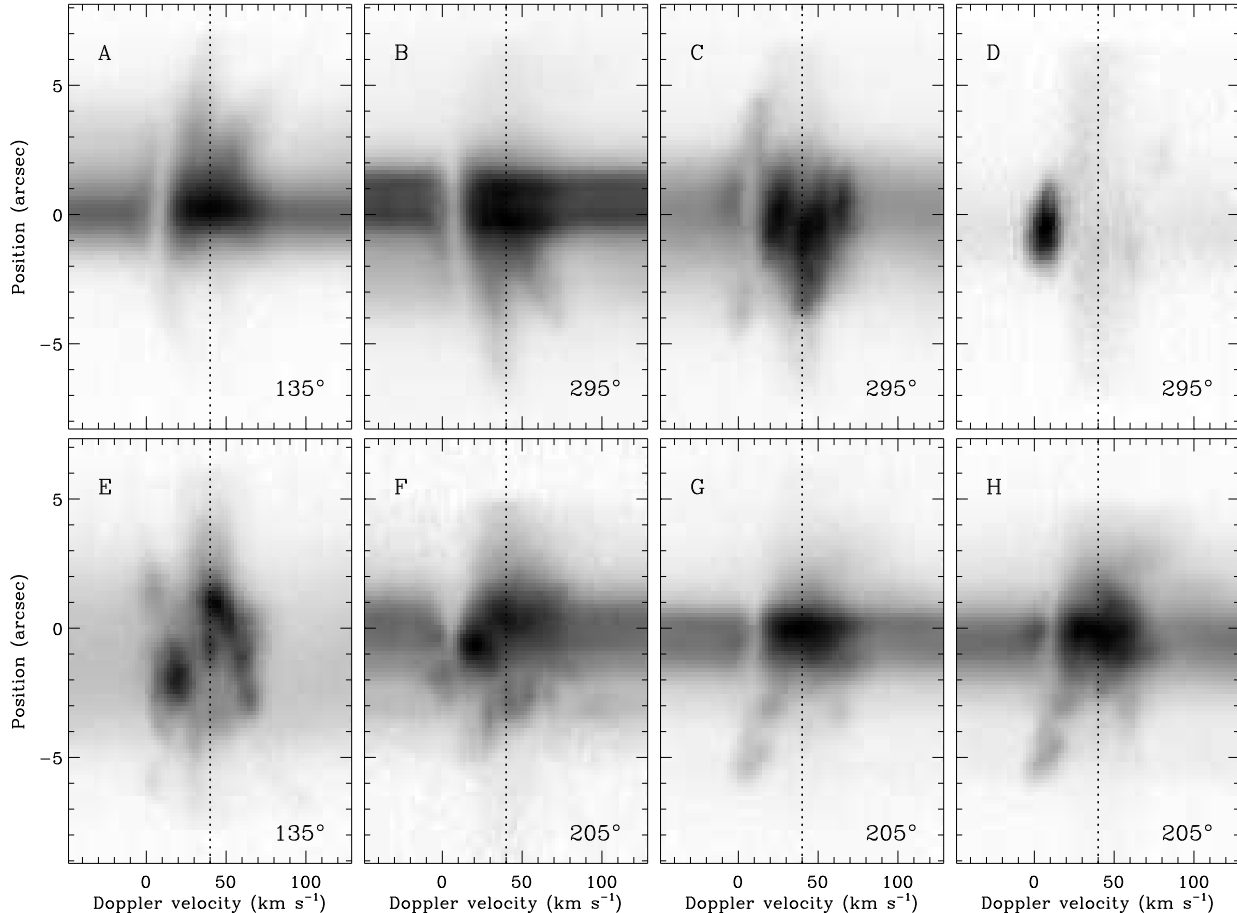


**Figure 2.** Position-velocity diagrams of K I  $\lambda 7699$  emission from the nebula of VY CMa. Panels A through H correspond to slit positions A through H labeled in Figure 1b. The upward direction on each panel in this figure corresponds to the position of the label A through H in Figure 1b, and down in each panel corresponds to the position angle given in the lower right and listed in Table 1. Heliocentric Doppler velocity is indicated on the X-axis, and the dashed vertical line marks the presumed systemic velocity of  $+40 \text{ km s}^{-1}$ . The full slit length of  $\sim 13''$  is slightly shorter than the range of position shown here.

the other K I line at  $7665 \text{ \AA}$  is strongly affected by absorption in the atmospheric A-band, and no other line in the spectrum had comparable brightness in the ejecta. Figure 2 shows the resulting position-velocity diagrams for K I  $\lambda 7699$  at the various slit orientations in Figure 1b.

### 3 DISCUSSION

The observations presented here were exploratory, and the most significant result is the discovery of bright *intrinsic* K I emission from the nebula around VY CMa — this extended K I emission is not simply a dusty reflection of the star’s K I emission line, but rather, it is intrinsic emission from the gas in the nebula itself.<sup>1</sup> It is therefore a powerful diagnostic of the kinematics and geometry of the extended

nebula. Inferring quantities like column densities and mass-loss rates from the K I emission requires detailed modeling beyond the scope of this short Letter (see the models of K I emission for the nebula of Betelgeuse; Jura & Morris 1981; Rodgers & Glassgold 1991; Glassgold & Huggins 1986), but the information provided here can hopefully be useful in such an investigation. A qualitative description of the data is given here, and some clues to the kinematics and geometry of the nebula are discussed. Figure 3 shows spectral intensity tracings at a few selected positions, and Table 2 collects some measurements from these tracings, such as the flux-weighted centroid velocity ( $v_{\text{cen}}$ ), the emission equivalent width (EW), the flux ratio of reflected continuum to the central star’s continuum ( $F/F_*$ ), and the intensity ratio of the extended K I emission compared to the emission line seen in the star ( $I/I_*$ ). Uncertainty in  $I/I_*$ ,  $F/F_*$ , and the EW is a few percent, or as much as  $\pm 10\%$  in the faintest outer “halo” spectrum. The values for EW,  $F/F_*$ , and  $I/I_*$  in Table 2 were corrected for instrumental scattering using observed values of  $F/F_*$  for a point source.

<sup>1</sup> This is immediately apparent because some of the emission is blueshifted, whereas reflection by expanding dust can only cause redshifted emission. A salient example is the Homunculus nebula around  $\eta$  Carinae (Smith et al. 2003).

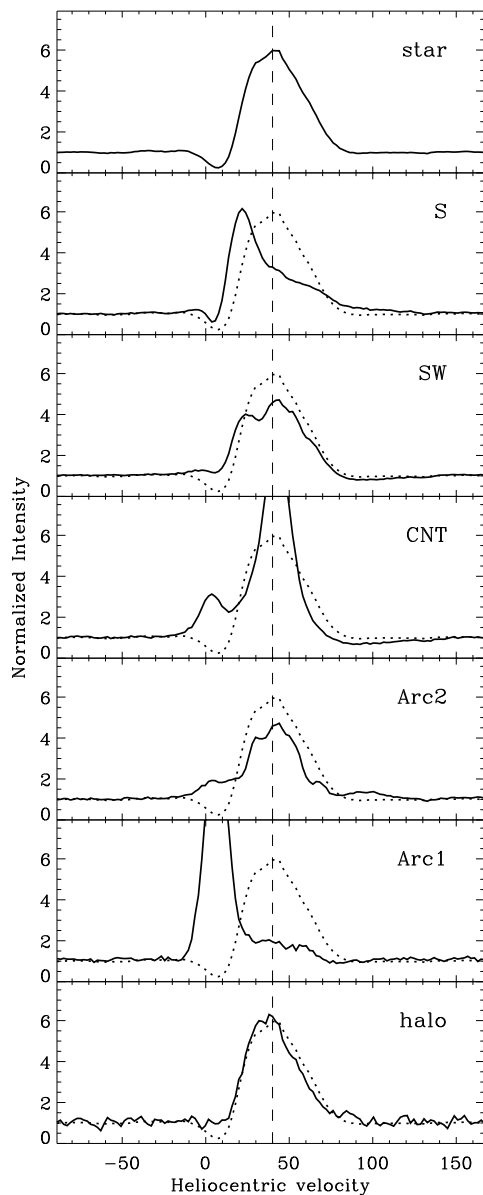


**Figure 3.** Intensity tracings of K I  $\lambda 7699$  at selected positions in the nebula. Names correspond to features labeled in Figure 1a; the “halo” spectrum is the average of several different positions in the nebula sampled from near the ends of the slit. All spectra have been normalized, for comparison with the star’s spectrum (shown with a dotted line in each panel). The heliocentric systemic velocity of  $+40.0 \text{ km s}^{-1}$  is shown with a dashed line.

### 3.1 Kinematic Structure

Examining Figures 2 and 3, it is obvious that the kinematic structure of K I  $\lambda 7699$  in VY Cma’s circumstellar nebula is complex, and not easily explained by spherical or axial symmetry. This is consistent with qualitative inspection of *HST* images of the nebula, which suggest either highly asymmetric mass ejection or selective extinction (or both; Smith et al. 2001; Kastner & Weintraub 1998). In general, bright K I emission with strong Doppler shifts is confined to within

**Table 2.** Measurements from spectral tracings

Feature	Radius (arcsec)	$v_{\text{cen}}$ ( $\text{km s}^{-1}$ )	EW ( $\text{\AA}$ )	F/F <sub>*</sub> (cont.)	I/I <sub>*</sub> (line)
star	...	+41.5	4.75	1	1
S	1	+32.4	4.02	0.13	0.11
SW	1	+41.0	3.33	0.10	0.07
CNT	3	+39.2	6.53	0.024	0.033
Arc2	3	+40.1	3.96	0.030	0.025
Arc1	5	+7.7	5.27	0.0083	0.0092
halo	6	+40.0	4.66	0.0014	0.0014

about  $5''$  from the star, and strong emission features can usually be associated with knots or filaments in images of the nebula (Figure 1). Many positions show multiple velocity components along the same line of sight, especially the bright knots like S and SW. The curved nebulous tail (CNT; see Herbig 1972) shows interesting kinematic structure (see slit position E in Figure 2, which runs along the CNT). Near the star it is redshifted by about  $20 \text{ km s}^{-1}$  (compared to  $v_{\text{sys}}$ ), and this Doppler shift gradually decreases to match  $v_{\text{sys}}$  at the apex of the CNT farthest from the star. Thus, the CNT might either be a bubble like Arc1 moving near the plane of the sky, or an expanding equatorial ring. Overall, the material with strong K I emission and chaotic kinematic structure is seen mainly toward the southwest of the star, in the brightest part of the reflection nebula.

Self absorption is not uniformly distributed either. Blueshifted absorption is seen in the bright central parts of the nebula near the star, and is concentrated toward the north and northeast. Ratio images also showed enhanced reddening toward the northeast (Smith et al. 2001). No absorption is seen more than  $1''$  from the star toward the southwest direction. The narrow absorption shows a velocity gradient with position: It shifts from about  $+20 \text{ km s}^{-1}$  (heliocentric) at a few arcseconds northwest of the star, reaching almost  $0 \text{ km s}^{-1}$  at positions a few arcsec east of the star.

While the faint outer halo has an emission profile almost identical to that of the star (Figure 3), the P Cyg absorption component is missing. The K I equivalent width in the halo is also nearly identical to the star (Table 2), so at large radii this halo is probably a pure reflection nebula. However, the missing P Cyg absorption component indicates that other lines of sight do not see the P Cyg absorption. Either the stellar wind of VY Cma is asymmetric, or the absorption is not a “real” P Cyg component formed in the wind, but is instead localized self absorption in the nebula.

### 3.2 Systemic velocity

At more than  $5''$  from the star in most position-velocity diagrams in Figure 2, a very faint emission component is seen at nearly the same velocity as that of the star. Images of VY Cma reveal a faint, fairly uniform scattering halo extending beyond  $5''$  from the star as well (Smith et al. 2001). Figure 3 shows an average of several different positions in this outer halo. This is not simply instrumental scattering of the bright star, because the P Cyg absorption is missing in the outer parts. This outer halo may be the best tracer of the systemic velocity of VY Cma. Table 2 gives the flux-weighted centroid velocity of K I in the halo, indicating a

likely systemic velocity of  $+40.0 \pm 1.5$  km s $^{-1}$  (heliocentric), or  $+21$  km s $^{-1}$  (LSR). This agrees with various other indicators of VY CMa's systemic velocity, varying between  $+37$  and  $+44$  km s $^{-1}$  (Wallerstein 1986; Bowers et al. 1983; Deguchi et al. 1983; Reid & Dickinson 1976; Neufeld et al. 1999; Harwit & Bergin 2002), and is close to the systemic velocity of molecular clouds associated with the nearby cluster NGC 2362 ( $+18$  km s $^{-1}$  LSR; Lada & Reid 1978).

### 3.3 Episodic ejection

Deep *HST* images of VY CMa revealed a filamentary arc about  $5''$  southwest of the star (Arc 1 in Figure 1a) that provoked speculation about asymmetric, episodic mass ejection due to stellar activity (Smith et al. 2001). Slit positions D, G, and H in Figure 1b were placed to study the velocity structure of Arc 1, and the results are striking. K I emission associated with Arc 1 is strongly blueshifted. Interestingly, it seems to show a quasi-Hubble law, perhaps composed of several clumps seen best in Figure 2 G and H. Its blueshift increases with separation from the star, reaching a maximum of about  $-40$  km s $^{-1}$  with respect to the star at a separation of  $5''$ . (The emission feature at  $-3''$  and  $+60$  km s $^{-1}$  in Figure 2 G and H may be Arc 2, consistent with the high reddening of Arc 2 in images; see Smith et al. 2001.) A Hubble-like flow would imply a single ejection episode, strengthening the hypothesis that Arc 1 is due to an asymmetric eruption from the star's surface.

The pseudo 'Hubble constant' for this flow is roughly  $-7.2$  km s $^{-1}$  arcsec $^{-1}$ . Without proper motions, the projection angle out of the plane of the sky  $\psi$  is unknown, but at a distance of 1.5 kpc, the observed velocity structure implies an age of  $t \approx 1000/(\tan \psi)$  years.

The spatial extent of the K I emission associated with Arc 1 suggests that the emission line originates mainly in the filled *interior* of a bubble outlined by Arc 1. Perhaps reflected light in images traces a thin filamentary dust shell swept up by the expanding gas emitting K I.

### 3.4 Comparison with Betelgeuse

Neutral potassium emission has been observed in the circumstellar environment of Betelgeuse as well, out to radii of roughly  $50''$  (Plez & Lambert 2002), whereas the brightest K I reaches roughly  $5''$  from VY CMa. Since VY CMa is about 10 times farther away, the actual radial extent of the K I emission is comparable around these two stars. However, the K I in VY CMa's circumstellar shell is much brighter with respect to the star;  $I/I_*$  is a factor of  $10^3$  to  $10^4$  stronger in VY CMa. Note that Betelgeuse shows no K I emission in the direct stellar spectrum, so Plez & Lambert measured  $I_*$  as the continuum flux in a  $1\text{-}\text{\AA}$  bin; thus,  $I/I_*$  in Table 2 needs to be multiplied by a factor of 4.75 (the EW of K I  $\lambda 7699$  for the star) for direct comparison with Betelgeuse. This relatively bright extended K I emission is partly due to the fact that direct photospheric light from VY CMa is obscured by its own circumstellar dust (Smith et al. 2001; Kastner & Weintraub 1998; Herbig 1972). Perhaps even the "stellar" K I emission arises in unresolved circumstellar ejecta, but appears so strong because the star is occulted. This may help explain the mystery of the unusually-bright

K I emission from VY CMa. However, understanding the physical conditions in the gas that gives rise to the bright K I emission, the potassium abundance, the mass-loss rate, and other properties will require quantitative modeling of the observed nebular spectrum.

### ACKNOWLEDGMENTS

Support was provided by NASA through grant HF-01166.01A from the Space Telescope Science Institute, which is operated by the Association of Universities for Research in Astronomy, Inc., under NASA contract NAS 5-26555. I thank an anonymous referee for helpful comments.

### REFERENCES

- Benson, J.M., & Mutel, R.L. 1979, *ApJ*, 233, 119  
 Benson, J.M., & Mutel, R.L. 1982, *ApJ*, 253, 199  
 Bernat, A.P., & Lambert, D.L. 1976, *ApJ*, 210, 395  
 Bernat, A.P., Honeycutt, R.K., Kephart, J.E., Gow, C.E., Sandford, M.T., & Lambert, D.L. 1978, *ApJ*, 219, 532  
 Bowers, P.F., Johnston, K.J., & Spencer, J.H. 1983, *ApJ*, 274, 733  
 Buhl, D., Snyder, L.E., Lovas, F.J., & Johnson, D.R. 1974, *ApJ*, 192, L97  
 Deguchi, S., Good, J., Fan, Y., Mao, X., Wang, D., & Ukita, N. 1983, *ApJ*, 264, L65  
 Glassgold, A.E., & Huggins, P.J. 1986, *ApJ*, 306, 605  
 Harwit, M., & Bergin, E.A. 2002, *ApJ*, 565, L105  
 Herbig, G.H., 1972, *ApJ*, 172, 375  
 Humphreys, R.M. 1970, *PASP*, 82, 1158  
 Hyland, A.R., Becklin, E.E., Neugebauer, G., & Wallerstein, G. 1969, *ApJ*, 158, 619  
 Jura, M., & Morris, M. 1981, *ApJ*, 251, 181  
 Kastner, J.H., & Weintraub, D.A. 1998, *AJ*, 115, 1592  
 Knowles, S.H., Mayer, C.H., Cheung, A.C., Rank, D.M., & Townes, C.H. 1969, *Science*, 163, 1055  
 Lada, C.J., & Reid, M.J. 1978, *ApJ*, 219, 95  
 Marvel, K.B. 1997, *PASP*, 109, 1286  
 Maun, N., Fort, B., Querci, F., Dreux, M., Fauconnier, T., & Lamy, P. 1984, *A&A*, 130, 341  
 Monnier, J.D., Tuthill, P.G., Lopez, B., Cruzalebes, P., Danchi, W.C., & Haniff, C.A. 1999, *ApJ*, 512, 351  
 Morris, M., & Bowers, P.F. 1980, *AJ*, 85, 724  
 Neufeld, D.A., Feuchtgruber, H., Harwit, M., & Melnick, G.J. 1999, *ApJ*, 517, L147  
 Plez, B., & Lambert, D.L. 1994, *ApJ*, 425, L101  
 Plez, B., & Lambert, D.L. 2002, *A&A*, 386, 1009  
 Reid & Dickinson 1976  
 Richards, A.M.S., Yates, J.A., & Cohen, R.J. 1998, *MNRAS*, 299, 319  
 Rodgers, B., & Glassgold, A.E. 1991, *ApJ*, 382, 606  
 Rosen, B.R., Moran, J.M., Reid, M.J., Walker, R.C., Burke, B.F., Johnston, K.J., & Spencer, J.H. 1978, *ApJ*, 222, 132  
 Smith, N., Davidson, K., Gull, T.R., Ishibashi, K., & Hillier, D.J. 2003, *ApJ*, 586, 432  
 Smith, N., Humphreys, R.M., Davidson, K., Gehrz, R.D., Schuster, M., & Krautter, J. 2001, *AJ*, 121, 1111  
 van Blerkom, D., & Auer, L. 1976, *ApJ*, 204, 775  
 Wallerstein, G. 1958, *PASP*, 70, 479  
 Wallerstein, G. 1986, *A&A*, 164, 101  
 Wallerstein, G., & Gonzalez, G. 2001, *PASP*, 113, 954